CellPress

Cell Host & Microbe
Article

IFITM Proteins Incorporated into HIV-1 Virions Impair Viral Fusion and Spread

Alex A. Compton,[1,2,*] Timothée Bruel,[1,2] Françoise Porrot,[1,2] Adeline Mallet,[3] Martin Sachse,[3] Marine Euvrard,[1,4] Chen Liang,[5] Nicoletta Casartelli,[1,2] and Olivier Schwartz[1,2,6,*]

[1]Institut Pasteur, Department of Virology, Virus & Immunity Unit, Paris 75015, France
[2]CNRS URA 3015, Paris 75015, France
[3]Institut Pasteur, Imagopole, Ultrastructural Microscopy Platform, Paris 75015, France
[4]École Normale Supérieure, Department of Biology, Cachan 94230, France
[5]Lady Davis Institute, McGill AIDS Centre, Montreal, QC H3T 1E2, Canada
[6]Vaccine Research Institute, Creteil 94010, France
*Correspondence: alex.compton@pasteur.fr (A.A.C.), schwartz@pasteur.fr (O.S.)
http://dx.doi.org/10.1016/j.chom.2014.11.001

SUMMARY

The interferon-induced transmembrane (IFITM) proteins protect cells from diverse virus infections by inhibiting virus-cell fusion. IFITM proteins also inhibit HIV-1 replication through mechanisms only partially understood. We show that when expressed in uninfected lymphocytes, IFITM proteins exert protective effects during cell-free virus infection, but this restriction can be overcome upon HIV-1 cell-to-cell spread. However, when present in virus-producing lymphocytes, IFITM proteins colocalize with viral Env and Gag proteins and incorporate into nascent HIV-1 virions to limit entry into new target cells. IFITM in viral membranes is associated with impaired virion fusion, offering additional and more potent defense against virus spread. Thus, IFITM proteins act additively in both productively infected cells and uninfected target cells to inhibit HIV-1 spread, potentially conferring these proteins with greater breadth and potency against enveloped viruses.

INTRODUCTION

Viruses, as obligate intracellular parasites, seize control of various compartments of the host cell to complete their life cycle. Viral replication requires the recruitment of cellular cofactors as well as the evasion of cell-intrinsic immune effectors that protect nearly every cellular niche from viral invasion. These antiviral factors, known as host restriction factors, reside in the cytoplasm, the nucleus, the plasma membrane, and the viral particle itself. The localization of restriction factors in the cell often corresponds to the step of the virus life cycle with which it interferes. For example, the nuclear dNTPase SAMHD1 depletes the pool of nucleotide triphosphates needed for viral reverse transcription (Laguette and Benkirane, 2012), while Mx2 restricts a postentry event in the cytoplasm prior to integration (Haller, 2013). APOBEC3G becomes incorporated into nascent budding virions and hypermutates the viral genome (Malim and Bieniasz, 2012). Tetherin (or BST-2) traps virions to the plasma membrane, blocking their release (Malim and Bieniasz, 2012). Newcomers to this category of membrane-bound restriction factors are the interferon-induced transmembrane (IFITM) proteins.

The human genome encodes at least five IFITM proteins, including three members with reported antiviral activity (IFITM1, IFITM2, and IFITM3) (Brass et al., 2009; Diamond and Farzan, 2013; Perreira et al., 2013; Smith et al., 2014). The antiviral IFITM proteins are nearly ubiquitously expressed and are further upregulated by type I interferons (IFN) (Siegrist et al., 2011). IFITM5 expression is restricted to osteoblasts and is required for bone mineralization, while the function of IFITM10 is unknown (Diamond and Farzan, 2013). Residents of cellular membranes at the interior and exterior of the cell, IFITM1, IFITM2, and IFITM3 may represent the earliest acting restriction factors yet identified. Previous reports demonstrate that they block virus entry (Brass et al., 2009; Huang et al., 2011) at the level of virus-cell fusion by affecting the biophysical properties (Desai et al., 2014; Li et al., 2013) or composition (Amini-Bavil-Olyaee et al., 2013) of the cellular membranes in which they are found. These proteins display antiviral function against many enveloped viruses, including influenza A virus (IAV), West Nile virus, dengue virus, severe acute respiratory syndrome coronavirus, hepatitis C virus, and Ebola virus (Perreira et al., 2013). While the majority of studies have relied on in vitro infection systems, it is well established that IFITM3 restricts IAV infection in vivo. *Ifitm3*-deficient mice fail to clear infection by otherwise mild strains of IAV (Bailey et al., 2012; Everitt et al., 2012), while a polymorphism in human *ifitm3* is enriched in patients hospitalized for severe influenza disease (Everitt et al., 2012). IFITM proteins have also been reported to inhibit HIV-1 replication. IFITM2 and IFITM3 impact HIV-1 entry, while IFITM1 may act by additional mechanisms (Jia et al., 2012; Lu et al., 2011). However, the effect on HIV-1 entry is relatively modest and depends on the experimental system (Brass et al., 2009; Lu et al., 2011). Establishing IFITM proteins as bona fide restriction factors of HIV-1, or any virus, will require the use of relevant in vitro assays, as well as an understanding of if and how the virus evades or antagonizes this activity. Furthermore, since IFITM proteins also play roles in cell adhesion, antiproliferation, and signaling (Diamond and Farzan, 2013), it is important to identify additional functions that these proteins may perform during viral infection.

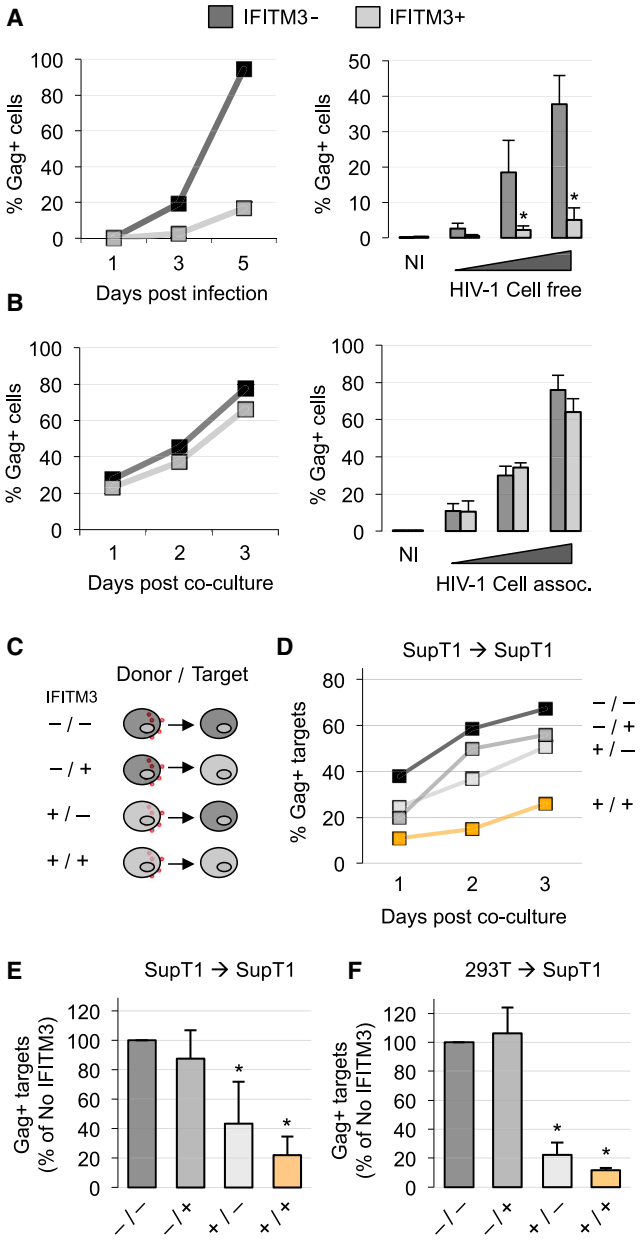

Figure 1. IFITM3 in Virus-Producing Cells Restricts HIV-1 Cell-to-Cell Transmission

(A) SupT1 cells were treated with doxycycline to induce FLAG-IFITM3 (see also Figure S1) before infection with NL4-3 HIV-1. Viral replication was followed by intracellular Gag staining at the days indicated. Left: one representative experiment. Right: mean ± SD of three independent experiments at day 3 p.i., with viral inoculum varying from 1 to 12 ng/ml p24.

(B) SupT1 cells were infected with NL4-3. When 30%–50% of the cells were Gag+, IFITM3 was induced, or not induced, overnight with doxycycline. These donor cells were cocultivated 2 hr with labeled SupT1 target cells expressing or not expressing IFITM3. Target cells were sorted, and transmission was monitored by the fraction of Gag+ target cells at the days indicated. Left: one representative experiment. Right: mean ± SD of three independent experiments at day 2 p.i., with increasing amounts of infection among donor cells, varying from 30% to 50%.

(C) Schematic illustration of the four combinations of cells tested.

(D) One representative experiment. Cocultures were performed as described in (B).

(E) Mean ± SD of three independent experiments at day 2 p.i.

(F) 293T cells were transfected with pNL4-3 and FLAG-IFITM3 expression plasmids and cocultivated with SupT1 target cells expressing or not expressing IFITM3 for 2 hr. Target cells were harvested, and transmission was monitored by measuring the fraction of Gag+ target cells. Mean ± SD of four independent experiments at day 2 p.i. Levels of Gag in the target cells in the absence of IFITM3 in both donors and targets were normalized to 100%. A one-sample t test was performed in (E) and (F), *$p < 0.05$. Comparisons were made between the condition indicated and the IFITM3$^{-/-}$ condition. See also Figure S1.

Using an in vitro coculture system designed to measure virus spread between lymphocytes, we report anti-HIV functions of IFITM proteins in virus-producing cells. IFITM proteins present in the uninfected cell are poorly effective at blocking HIV-1 entry, yet in cells that are already infected, they incorporate into virions and diminish virus infectivity. We demonstrate that IFITM proteins exert their anti-HIV activity most potently from within the virus membrane. Thus, this class of restriction factor impinges on the viral life cycle of HIV-1, and possibly other enveloped viruses, at multiple steps.

RESULTS

Revealing the Antiviral Potential of IFITM Proteins in Virus-Producing Cells

While the role of IFITM proteins as inhibitors of virus entry is well established, the experimental systems used to characterize this antiviral function have relied on cell-free virus infections (Smith et al., 2014). However, HIV-1 spreads effectively in culture and likely within infected individuals by passing directly between cells in a process known as cell-to-cell transmission (Dale et al., 2013; Sattentau, 2011; Sourisseau et al., 2007; Murooka et al., 2012). We used previously described doxycycline-inducible CD4+ SupT1 T cell lines (Figure S1A, available online), engineered to allow expression of FLAG-IFITM3, to describe their effect during HIV-1 replication. In these cells, a fraction of IFITM3 is found at the cell surface, as assessed by flow cytometry (Figure S1B).

As reported (Lu et al., 2011), induction of IFITM3 in target cells followed by incubation with cell-free virions resulted in a potent block to viral replication (Figure 1A). However, increasing the viral inoculum lead to a less marked restriction (Figure S1C), suggesting that this antiviral effect may be partly saturable. We then assessed the ability of IFITM to impact direct viral cell-to-cell spread. We used a transient coculture system (Malbec et al., 2013; Sourisseau et al., 2007), in which HIV-1-infected donor T cells were mixed with dye-labeled SupT1 target cells. After 2 hr of coculture, target cells were isolated using a cell sorter. Infection of target cells was assessed up to 3 days later by measuring Gag expression (Figure 1B). The Gag signal in targets was due to de novo synthesis, since it was significantly reduced in the presence of reverse transcriptase inhibitor Nevirapine (data not shown). In contrast to cell-free HIV-1, when infections were performed by coculture, the induction of IFITM3 in target cells had little to no effect on inhibiting virus spread (Figure 1B). This lack of antiviral effect was observed when donor cells were infected at different levels (Figure 1B). Thus, IFITM3-expressing cells are no longer protected against infection from

cell-associated virus, partly because local titers using virus-producing cells are high. This led us to ask whether IFITM3 possesses other antiviral functions that are robust to this mode of HIV spread. We modified the coculture system to include conditions in which IFITM3 was induced either in infected donors, in targets, or in both (Figure 1C). While IFITM3 in uninfected target cells had minimal effect, IFITM3 in the donors decreased HIV transmission approximately 2-fold (Figures 1D and 1E). A more potent inhibition was observed when both donors and targets expressed IFITM3, which resulted in a 5-fold decrease in productive target cell infection. This unexpected role of IFITM3 was confirmed using another coculture system in which the virus does not spread in the donor cells. We cotransfected 293T cells with an HIV-1 provirus and an IFITM3-expressing plasmid and cocultured them with IFITM3-negative or -positive SupT1 cells. A 5-fold inhibition of virus transmission to target cells was observed in this system, and inhibition was further enhanced when target cells also expressed IFITM3 (Figure 1F). Titration of the *ifitm3*-encoding plasmid demonstrated that inhibition of transmission was dependent on the amount of IFITM3, while a control plasmid encoding MxA had no effect (Figure S1D).

Together, these coculture experiments identify that HIV-1, by spreading intercellularly, escapes canonical IFITM-mediated restriction in the uninfected target cell. However, IFITM proteins potently inhibit the spread of virus from cells that are already infected.

Real-Time Analysis of the Impact of IFITM3 on HIV-1 Cell-to-Cell Spread

To further document the effect of IFITM3, we performed a dynamic analysis of viral spread, using HIV-1 encoding an IRES GFP cassette (Wildum et al., 2006). Infected SupT1 cells were mixed with target SupT1 cells expressing an RFP marker. Cells were then plated in microdishes coated with fibronectin and visualized by time-lapse fluorescence microscopy with images acquired every 5 min for up to 60 hr. Representative examples of viral spread, in the absence of IFITM3 or with IFITM3 expressed in both donors and targets, are shown in Movie S1. Time-lapse analysis showed that in the absence of IFITM3, HIV-1 efficiently spread to new targets, measured as double GFP+ RFP+ objects (Figures 2A and S2A). IFITM3 significantly impaired viral propagation, with a 4-fold decrease in the number of newly infected target cells after 60 hr of continuous coculture (Figure 2A). As expected, an Env-defective virus (HIV-1ΔEnv) did not spread to new recipients (Figure 2A), and Nevirapine abrogated viral replication (data not shown). Cells were interrogated at the end of the coculture by flow cytometry to confirm the effect of IFITM3 on viral spread (Figure S2B). We then visually scored the appearance of syncytia, identified as giant GFP+RFP+ cells eventually displaying bubble-like membrane extensions (Figure 2C). IFITM3 strongly decreased the number of syncytia observed, a phenomenon previously attributed to IFITM proteins in the context of other viruses (Li et al., 2013; Lin et al., 2013) (Figures 2B and 2C). Image extraction at different time points demonstrated that in the presence of IFITM3, infected donor GFP+ cells formed clusters with target RFP+ cells, but in most cases these structures did not lead to cell fusion (Figures 2B and 2C). We also performed a time-lapse microscopy analysis of viral spread when IFITM3 was induced in donors or in targets alone. The main antiviral effect was observed when IFITM3 was present in the donor cells (Figure S2C). Therefore, the inhibitory effect of IFITM3 on HIV-1 cell-to-cell transmission is associated with a significant decrease of fusion between infected and target cells, suggesting a decrease in virus production from infected cells and/or a defect in the fusion capacity of membranes present at cell-cell contacts.

IFITM3 Diminishes Virus Infectivity and Incorporates into Virions

To uncover the mechanisms involved in this restriction, we studied the impact of expressing IFITM3 in productively infected cells. In SupT1 cells, overnight induction of IFITM3 following infection resulted in moderately decreased levels of intracellular Gag and surface Env proteins, as measured by the mean fluorescence intensity of these two proteins in a fraction of infected cells (Figure 3A). This slight decrease may be the result of IFITM3 preventing viral spread to new targets or of a direct effect of IFITM3 on the production or stability of these viral proteins. Accordingly, the amount of Gag antigen detected in the supernatants was decreased (Figure 3B).

Notably, virus recovery from the supernatants, followed by sucrose purification, normalization to p24 antigen, and infection of fresh SupT1 target cells, revealed that IFITM3 proteins strongly reduced virion infectivity; virus produced from IFITM3-expressing infected cells was 4–5 times less infectious (Figure 3C). The decrease in infectivity was 2-fold when virions were tested on HeLa-CD4 reporter cells (Figure S3A). HIV-1 likely utilizes different entry pathways when infecting T cells or HeLa-CD4 cells, and this may affect virus sensitivity to restriction by IFITM3.

To further describe the effect of IFITM3 on infectivity, we analyzed virion content. When IFITM3 was present in the virus-producing cell, it was detected in released virus particles, purified by a double ultracentrifugation through sucrose and Optiprep cushions (Figure 3D). IFITM3 also cosedimented with Gag proteins when viral particles were highly purified on a 6%–18% Optiprep velocity gradient to discriminate between virus particles and microvesicles (Figure S3B). Notably, IFITM3 did not affect the levels of viral envelope glycoproteins incorporated into virions (Figure 3D). Detergent treatment, to strip away the viral membrane (Accola et al., 2000), removed the membrane-associated p17 Gag (MA), as well as IFITM3, while viral core protein p24 Gag (CA) remained (Figure 3D). This strongly suggests an association of IFITM3 with the viral membrane rather than with the core.

We then performed a dose-response analysis of the antiviral effect of IFITM3. By incrementally increasing IFITM3 protein levels in 293T cells, we observed increasing amounts of IFITM3 incorporated into virions, correlating with a decrease in particle infectivity (Figure 3E). Levels of Gag in 293T cells, as well as Gag released in supernatants, were minimally affected by IFITM3 expression (Figure S3C). To provide further evidence of IFITM3 incorporation into virus particles, virus prepared in the presence or absence of IFITM3-FLAG was immunolabeled with anti-FLAG and protein A-gold. Immunogold labeling revealed specific detection of IFITM3 at or close to the virion surface (Figures 3F and S4A).

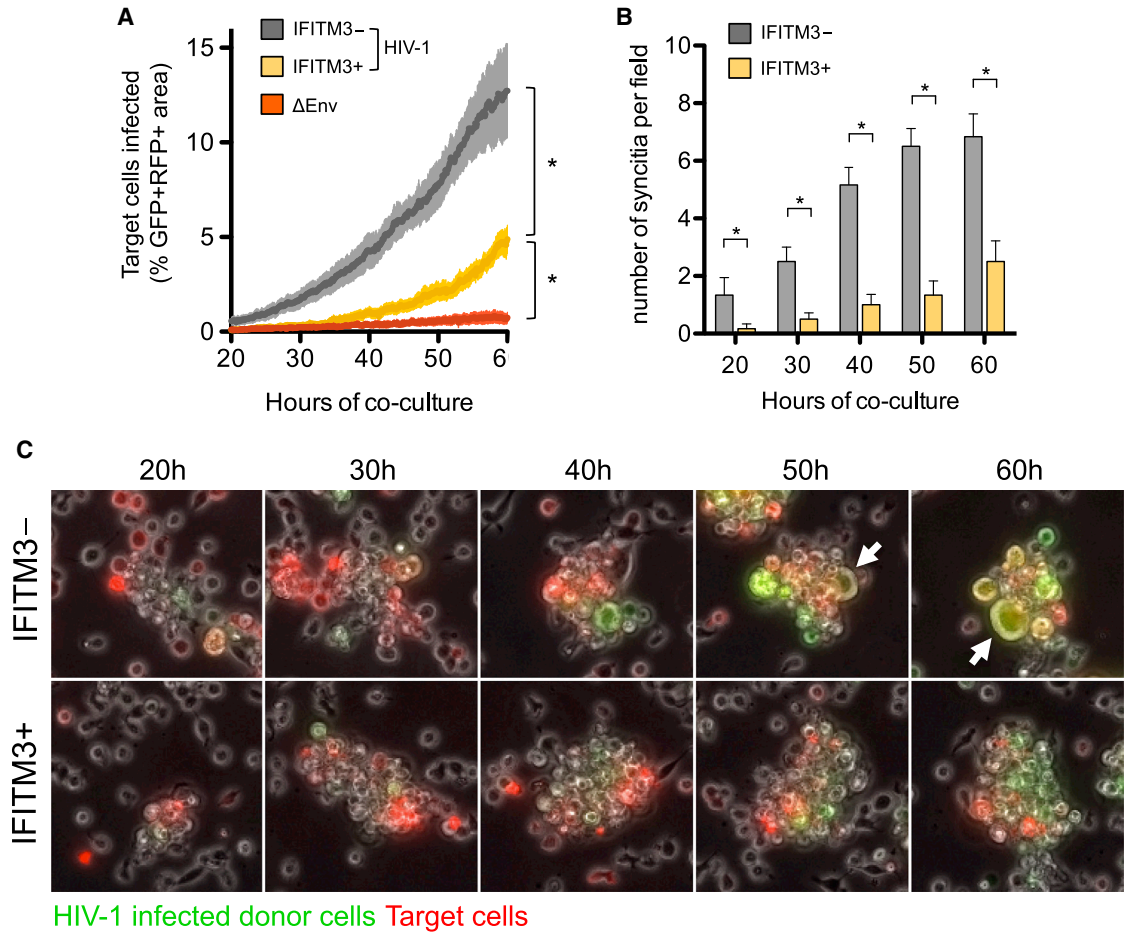

Figure 2. Real-Time Video Microscopy Analysis of HIV-1 Spread and Syncytia Formation

(A) SupT1 cells were infected by HIV-IRES-GFP/VSV or HIVΔEnv-IRES-GFP/VSV for 2 days. FLAG-IFITM3 was then induced or not induced in infected cells. These cells were adjusted for Gag+ levels and mixed with target SupT1-actin-mRFP cells, expressing or not expressing IFITM3. Images were taken every 5 min for 60 hr. The area of GFP and RFP colocalized pixels was quantified and used as a marker of target cell infection. Six fields in two independent experiments were analyzed and plotted as mean ± SEM. See Movie S1 for a representative time-lapse and Figure S2 for flow cytometry analysis of the experiment.

(B) Clearly identifiable, oversized infected cells were considered as syncytia and visually scored at the indicated time points. Six fields in two experiments were analyzed and plotted as mean ± SEM.

(C) Images extracted from Movie S1 were extracted at the indicated time points and centered on a cell cluster. White arrows indicate examples of syncytia. Mann-Whitney test, *$p < 0.05$. See also Movie S1 and Figure S2.

Endogenous IFITM Proteins Restrict HIV-1 Cell-to-Cell Transmission

Our experiments show that the ectopic expression of IFITM3 in virus-producing SupT1 lymphocytes and 293T cells restricts viral spread. We used HeLa cells to address whether endogenous IFITM proteins also exhibit this antiviral potential. Flow cytometry analysis with two antibodies recognizing IFITM1 and IFITM2/IFITM3, respectively, indicated that HeLa cells naturally express IFITM2/3 and very little of IFITM1 (Lu et al., 2011). The expression of all three proteins was upregulated by type I IFN (Figure 4A). Furthermore, endogenous IFITM2/3 is incorporated into virions produced from HeLa cells, but not from 293T cells, which express only trace amounts of IFITM proteins (Figures S4B and S4C). We thus silenced the three *ifitm* genes by siRNA in type I IFN-treated cells (Figure 4A). These cells were infected with VSV-G pseudotyped HIV-1, and their ability to transmit infection was assessed by performing a coculture with SupT1 target cells. Knockdown of endogenous IFITM proteins resulted in a 2- to 3-fold increase in virus transmission to targets (Figure 4B) and the production of virions that were 3-fold more infectious (Figure 4C). Thus, endogenous IFITM proteins in infected cells limit viral cell-to-cell spread and reduce virion infectivity.

IFITM in Virus-Producing Cells Prevents Fusion between Virus and Target Cells

We next explored the mechanism by which IFITM3 in donor cells may diminish virion infectivity. As IFITM residing in endosomal membranes block the entry of many viruses at the stage of fusion, we predicted that IFITM localized to the viral membrane would have similar effects. To quantify HIV-1 entry, we used a virion fusion assay, which allows the discrimination between viral entry into the cytoplasm and endosomal capture

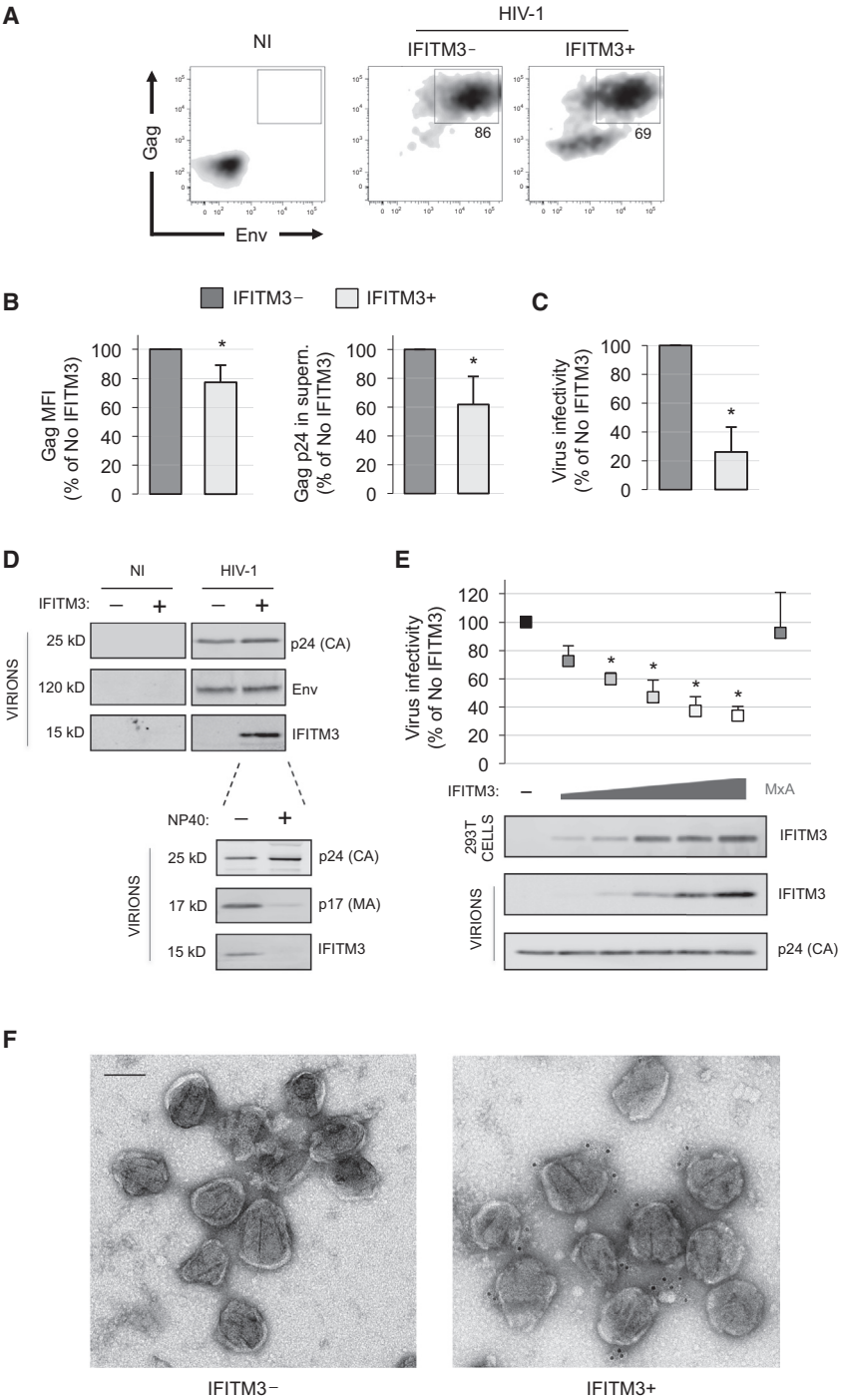

Figure 3. IFITM3 in Infected Cells Diminishes Virus Infectivity and Incorporates into Virions

(A) SupT1 cells were infected with HIV-1 for 48 hr and induced or not induced to express FLAG-IFITM3. Levels of HIV-1 Env at the surface and of intracellular Gag were measured by flow cytometry, with the percentage of Gag+Env+ cells notated. One representative experiment is shown.

(B) Left: the mean fluorescence intensity (MFI) of Gag was measured in the fraction of Gag+ cells. Right: Gag p24 antigen levels in the supernatants measured by ELISA. Gag MFI and p24 levels in the absence of IFITM3 were normalized to 100%. Mean ± SD of five independent experiments is shown.

(C) Viral supernatants from IFITM3 positive and negative SupT1 cells were tested for infectivity. Viral particles were purified, and the inoculum (adjusted for 25 ng p24) was added to fresh SupT1 cells. Infection was assessed by measuring the fraction of Gag+ cells after 2 days. Infection in the absence of IFITM3 was normalized to 100%. Mean ± SD of four independent experiments is shown (see also Figure S3A for infectivity assay on HeLa-CD4 cells).

(D) Viral particles from FLAG-IFITM3 positive and negative SupT1 cells were purified by a double ultracentrifugation on cushions of sucrose and Optiprep and analyzed by western blot. One representative experiment is shown, with 25 ng of p24 loaded in each lane and probed with anti-FLAG.

(E) 293T cells were cotransfected with a pNL4-3 provirus and with increasing doses of FLAG-IFITM3 expression plasmid. Viral particles released in supernatants were harvested, and infectivity was assessed on HeLa-CD4 cells, with 100% corresponding to virions produced without IFITM3. Mean ± SD of three independent experiments is shown. MxA expression plasmid was used as a control. Levels of IFITM3 in 293T cell lysates and purified virions are shown in the lower panels.

(F) Purified virus particles, produced in 293T cells cotransfected with pNL4-3 and either IFITM3-FLAG or control plasmid, were fixed and immunogold labeled with anti-FLAG. Representative fields are shown. Other fields are shown in Figure S4A. Scale bar, 100 nm. A Wilcoxon signed-rank test was performed on raw values in (B) and (C), and a one-sample t test was performed in (E); *p < 0.05. See also Figures S3 and S4.

(Cavrois et al., 2002; Roesch et al., 2012). This assay relies on the use of viruses containing a β-lactamase-Vpr (βlam-Vpr) protein chimera. The cytoplasmic access of βlam-Vpr as a result of fusion, after 2 hr of infection, is monitored by the enzymatic cleavage of CCF2-AM, a fluorogenic substrate of β-lactamase loaded in target cells. A typical experiment showed that virions produced in the presence of IFITM3 exhibited a marked defect for fusion with recipient SupT1 lymphocytes (Figure 5A). As a negative control, HIV encoding fusion-defective Env (HIV-1 F522Y) did not enter the cytoplasm (Figure 5A). Virions incorporating IFITM3 decreased the fusogenicity of virions by 5- to 10-fold (Figure 5B) using either SupT1 or MT4C5 T cell lines as targets. Analysis of Gag expression at a later time point (48 hr postinfection [p.i.]) confirmed that productive infection was strongly impaired in both target cells (Figure 5C). We then used viral particles produced in the presence of IFITM1, IFITM2, or IFITM3. The three proteins were individually incorporated into particles (Figure S5A), and all decreased viral fusion to different extents (Figure S5B). IFITM3 was the most potent, while IFITM1 and IFITM2 imposed a restriction of approximately 2-fold. An untagged version of

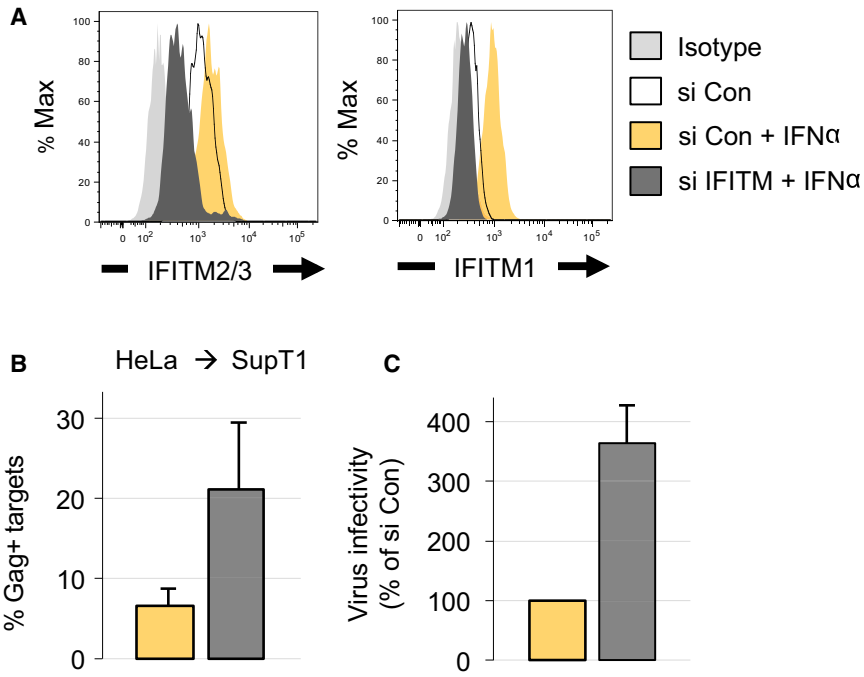

Figure 4. Endogenous IFITM Proteins in Infected Cells Inhibit the Spread of HIV-1

(A) HeLa cells were transfected with control siRNA (si Con) or with siRNA targeting the three IFITM (si IFITM) and treated with IFNα_{2a} for 48 hr. IFITM1 and IFITM2/3 levels were assessed by flow cytometry. A representative experiment is shown. (B and C) These cells were simultaneously infected with NL4-3 (VSV). Viral supernatants were harvested 48 hr later, and cells served as donors in a transmission assay. (B) HeLa cells were cocultivated with SupT1 targets for 2 hr, target cells were harvested, and transmission was monitored at day 2 p.i. Mean ± SD of three independent experiments. (C) Viral supernatants from silenced cells were measured for infectivity as described in Figure 3. Infection by virions produced in the si Con cells was normalized to 100%. Mean ± SD of three independent experiments is shown. Mann-Whitney test, *$p < 0.05$. See also Figure S4.

IFITM3 displayed a similar capacity to block virion fusion (Figure S5C).

We then analyzed fusion after cell-to-cell viral transfer. After 2 hr of coculture with βlam-Vpr-positive infected 293T donor cells, expressing or not expressing IFITM, we harvested SupT1 target cells and analyzed CCF2-AM cleavage. The three IFITM proteins, when present in donor cells, also inhibited viral fusion in this setting (Figure S5D).

It has been reported that cellular membrane-resident IFITM2 and IFITM3 in target cells partially decrease HIV-1 entry (Lu et al., 2011). Therefore, we tested how virion-incorporated IFITM3 compares with cellular IFITM3 with regards to blocking virus fusion by performing the fusion assay using SupT1 target cells expressing or not expressing IFITM3 (Figure 5D). An effect of IFITM3 in target cells was observed only when low doses of virus were used, confirming that restriction in the recipient lymphocyte is modest (Figure 5D). In contrast, the fusion of virus containing IFITM3 was strongly restricted, regardless of the viral inoculum used (Figure 5D). This effect was even greater when both virions and cellular membranes were expressing IFITM3. Thus, the effect of IFITM3 in target cells is saturable and exerts a relatively weak block to virus entry compared to the activity of virion-incorporated IFITM3. These results strongly suggest that IFITM proteins are dramatically more effective at restricting virus-cell fusion when localized to the viral membrane.

Endogenous IFITM Proteins Are Upregulated in Activated CD4+ T Cells and Incorporate into HIV-1 Virions during Infection

As the principal targets of HIV-1 infection in vivo, we measured the levels of endogenous IFITM proteins in primary CD4+ T cells and addressed how they are affected by cell activation status and type I IFN treatment. Nonactivated CD4+ T cells contained low, but detectable, levels of IFITM1 and IFITM2/3, with the former expressed to a higher extent (Figure 6A). Upon activation by phytohemagluttinin (PHA) and interleukin-2 (IL-2), IFITM levels were increased, consistent with a previous report showing IFITM induction upon T cell activation (Raposo et al., 2013). Addition of type I IFN further upregulated these proteins, with IFITM1 showing a greater degree of induction (Figure 6A). Staining without saponin permeabilization indicated that a fraction of IFITM proteins was present at the cell surface, with levels increasing upon type I IFN treatment (Figure S6B). The levels of IFITM proteins in type I IFN-treated CD4+ T cells were within the range of those observed in doxycycline-induced SupT1 T cells (data not shown).

We used confocal immunofluorescence microscopy to track the localization of IFITM2/3 in uninfected and infected primary CD4+ T cells. IFITM2/3 expression in the uninfected cell appeared primarily as small puncta distributed throughout the cytoplasm and partially colocalized with endosomal or lysosomal markers (transferrin receptor, CD63, and LAMP1/LAMP2), consistent with previous reports using nonlymphoid human cell lines (Amini-Bavil-Olyaee et al., 2013; Feeley et al., 2011; Weston et al., 2014) (Figure 6B and data not shown). Upon infection, the signal for IFITM2/3 protein appeared elevated and often shifted to a mostly perinuclear localization (Figure 6C). Interestingly, IFITM2/3 staining often colocalized with that of HIV-1 Env in the cell interior, while surface-associated IFITM2/3 could also be observed at probable virus budding sites containing both Env and Gag (Figure 6C). IFITM3 was also detected within virions produced from SupT1 cells expressing an Env-deleted HIV-1, indicating that IFITM3 can be incorporated through an Env-independent mechanism (Figure S6A). Costaining of IFITM1 and IFITM2/3 showed that the proteins display overlap in their distribution within HIV-1-infected cells and that IFITM proteins colocalize with viral Gag protein on the cell surface (Figure S6C).

By infecting primary, activated CD4+ T cells with primary HIV-1 isolates (DH12, Bx08, and BON strains), or the NL4-3

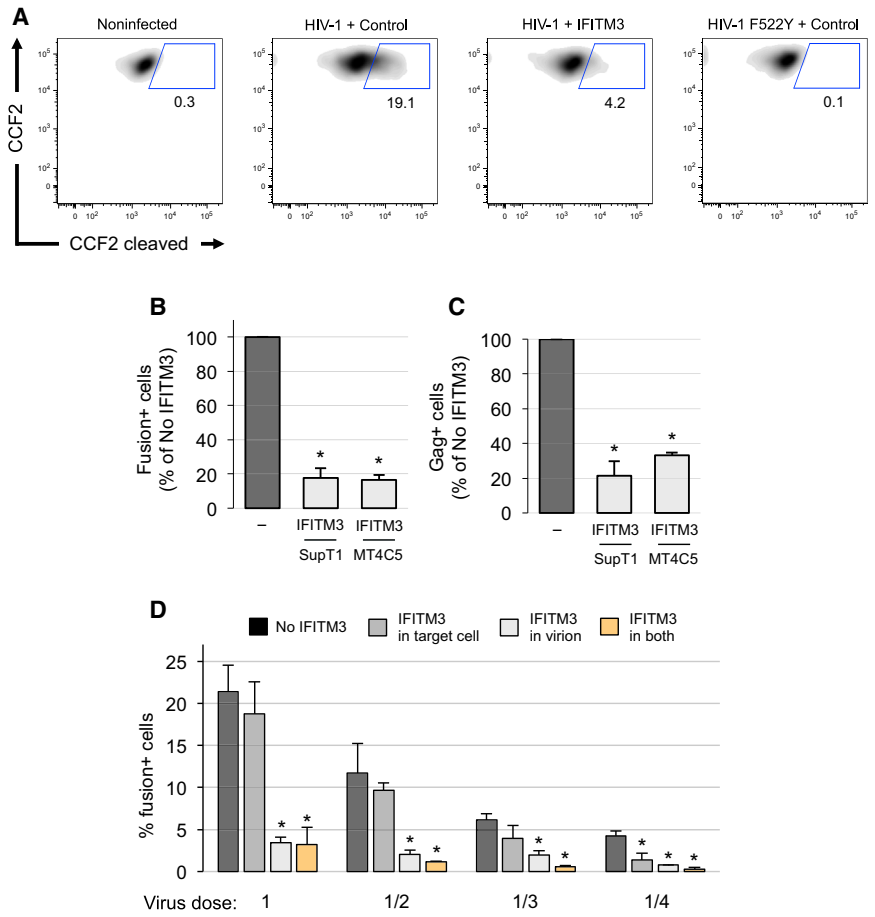

Figure 5. IFITM3-Containing Virions Are Poorly Fusogenic

(A) One representative test for viral fusion. SupT1 cells were exposed to virions containing Blam-Vpr, produced in the presence or absence of FLAG-IFITM3, for 2 hr at 37°C. Viral access to the cytoplasm was assessed by flow cytometry, using the cleavage of CCF2-AM as a readout. F552Y: non-fusogenic *env* mutant.

(B) Fusion of virions produced in the absence of IFITM3 was normalized to 100%. Two different target cells were used, SupT1 and MT4C5 cells. Mean ± SD of three independent experiments.

(C) Virions used for the fusion assay were also tested for their infectivity. Viral inoculum (adjusted for 25 ng p24) was added on fresh SupT1 or MT4C5 cells, and infection was assessed by Gag+ cells after 2 days. Infection by virions produced in the absence of IFITM3 was normalized to 100%. Mean ± SD of three independent experiments is shown.

(D) Virions produced as described in (A) were tested for fusion on target SupT1 cells expressing or not expressing IFITM3. A titration of the viral inoculum was performed, with the maximum dose corresponding to 25 ng Gag p24. Mean ± SD of three independent experiments is shown. Mann-Whitney test, *$p < 0.05$. Comparisons were made between the condition indicated and the No IFITM3 condition. See also Figure S5.

laboratory-adapted virus, we asked whether IFITM proteins were naturally incorporated into virions. Endogenous IFITM proteins were detected in purified viral particles (Figure 6D), with the extent of incorporation slightly varying between viral isolates. Therefore, IFITM proteins present in primary CD4+ T cells are capable of infiltrating virus particles. Notably, immature monocyte-derived dendritic cells (MDDCs) also expressed IFITM proteins, which were upregulated upon cellular maturation or by type I IFN (Figure S6D).

Altogether, our results show that endogenous IFITM proteins are found in primary T cells and MDDCs. In T cells, they colocalize with viral proteins and are incorporated into viral particles. Therefore, the antiviral functions of IFITM proteins described herein may be relevant for natural HIV-1 infections.

DISCUSSION

IFITM proteins belong to the CD225 protein superfamily, which can be found in nearly every domain of life, ranging from bacteria to invertebrates to primates. The array of *ifitm* genes in humans and other species most likely originated via tandem gene duplication events in our early vertebrate ancestors (Hickford et al., 2012; Siegrist et al., 2011). The expansion of *ifitm* loci suggests that the antiviral properties of IFITM, and possibly those of other CD225 proteins, have been selected and retained for protection against viral infections. Here, we describe a function of IFITM that may be important for its conservation over evolutionary time.

We show that HIV-1 cell-to-cell transmission allows the virus to bypass IFITM restriction in target cells. However, IFITM proteins limit the spread of virus from infected cells, at least in part by rendering virions less infectious and less fusogenic. Interestingly, while IFITM3 in uninfected lymphocytes has a minimal protective effect against HIV-1, it serves an additive antiviral role when IFITM3 is also present within incoming virions. The reason for this may lie with the accepted mechanism by which IFITM proteins inhibit the fusion capacity of membranes in which they reside. IFITM proteins inhibit steps leading to the formation of a fusion pore by increasing the curvature of cell membranes and reducing their fluidity (Desai et al., 2014; Li et al., 2013; Lin et al., 2013). If IFITM3 similarly contorts the viral membrane and causes similar biophysical consequences (Everitt et al., 2012) then the apposition of two IFITM3-containing membranes may make virus-cell fusion even more unlikely. Alternatively, IFITM incorporation into viral membranes may indirectly affect fusogenicity by excluding factors necessary for virus-cell fusion or by recruiting other inhibitors of this process. For example, while we did not detect differences in Env glycoprotein levels in virions containing or not containing IFITM3, Env conformation may be compromised. Although unlikely, this hypothesis deserves further investigation.

Despite that IFITM proteins may be localized to different cellular compartments in the absence of infection, with IFITM1 residing primarily at the plasma membrane (John et al., 2013; Mudhasani et al., 2013) and IFITM2 and IFITM3 residing in late endosomes and lysosomes (Amini-Bavil-Olyaee et al., 2013;

Feeley et al., 2011; Weston et al., 2014), we detect all of them in HIV-1 virions. This could be explained by the fact that all IFITM proteins transit, at least transiently, to the cell surface following translation (Chesarino et al., 2014; Jia et al., 2014; Weston et al., 2014). HIV-1 virion assembly is thought to occur primarily at the plasma membrane but may also occur in an intracellular compartment connected to the surface in some cell types, such as macrophages (Deneka et al., 2007; Jouve et al., 2007; Sundquist and Kräusslich, 2012; Welsch et al., 2007). Our confocal microscopy analysis of primary infected lymphocytes demonstrated a colocalization of IFITM proteins with viral proteins Env and (to a lesser extent) Gag. Targeting to lipid rafts, which have been shown to harbor IFITM1 (Perreira et al., 2013), is important for optimal virus release (Tang et al., 2009). Therefore, there are numerous potential meeting sites for the virus and IFITM within infected cells. Our time-lapse analysis of cell-to-cell transmission demonstrated a striking diminution of syncytia formation between IFITM3-expressing cells. Syncytia are likely the consequence of fusion events occurring at the plasma membrane. This further suggests that the surface of the productively infected cell is the main site at which IFITM3 exerts this antiviral function. We also observed an increase in cell surface-associated IFITM2/3 following IFN treatment. This complements published data indicating that IFN treatment or overexpression modifies IFITM localization (Brass et al., 2009; Perreira et al., 2013). Further work will aid in our understanding of how HIV-1 impacts IFITM localization. Interestingly, we showed here that Env is not required for IFITM3 incorporation into virions. Addressing the passive or active nature of IFITM association with virions will require the identification of virus strains or mutants that exhibit differential sensitivity to IFITM virion infiltration. Such differences, if they should exist, may lie in different strategies used by viruses to assemble and egress from the infected cell.

In uninfected cells, the protective effect of IFITM is dependent on their intracellular localization. The trafficking and localization of IFITM is regulated by sorting motifs within the N-terminal intracytoplasmic domain and by palmitoylated cysteine residues (Ding et al., 2014; Yount et al., 2010). IFITM function is also regulated by phosphorylation (Chesarino et al., 2014). It will be worthwhile to use various IFITM mutants to determine precisely where and how these proteins are incorporated into viral particles. We show here that IFITM proteins are expressed and upregulated by type I IFN in primary T lymphocytes and in DCs, two natural targets of HIV-1 in vivo. In these cells, as well as in macrophages, viral entry, budding, and egress pathways display notable differences. Further work will address the cell-type specificity of this restriction activity of IFITM.

Apart from our finding that IFITM proteins become incorporated into virus particles and decrease particle infectivity, we also observed that ectopic IFITM expression slightly decreases viral production. The presence of IFITM3 in infected SupT1 T cells or in transfected 293T cells resulted in modest decreases in HIV-1 Gag expression, consistent with articles reporting similar findings in these two cell types (Chutiwitoonchai et al., 2013; Ding et al., 2014; Lu et al., 2011). However, by introducing limiting amounts of IFITM3 in 293T, we observed an inhibition of virus transmission without affecting viral production. Therefore, we believe that the block in virus transmission conferred by IFITM3 is primarily the result of decreased viral infectivity and fusogenicity. It will also be worth determining whether IFITM proteins accumulate at or modify the formation of virological synapses between infected and uninfected T cells.

Now that we have expanded our understanding of how IFITM proteins contribute to intrinsic immunity, it will be important to study these functions in the context of other enveloped viruses. This analysis may reveal whether viruses sensitive to IFITM in the target cell are also susceptible to this donor cell-specific mode of antiviral function, i.e., virion incorporation and decreased infectivity. Furthermore, it will be important to address whether viruses previously described as IFITM-resistant (murine leukemia virus, arenaviruses) are in fact sensitive to this mode of inhibition. Furthermore, future experiments will require attention to the virus-producing cell type, especially the combination of donor and target cells used in experiments. Since IFITM proteins are known to form homo- and heteromultimers, and these interactions are necessary for full antiviral activity (John et al., 2013), combinatorial approaches must be employed to study their collective activity, in both the cell and the virion. Together, these approaches will reveal the full breadth and potency of IFITM proteins.

A recent report highlighted that HIV-1 can evolve resistance to IFITM1 in vitro through mutations in Env and Vpu proteins, with an effect of increasing viral fitness via enhancement of cell-to-cell spread (Ding et al., 2014). This concurs with our results showing that HIV-1 cell-to-cell transmission is less sensitive to IFITM-mediated restriction than cell-free virus infection. Viral cell-to-cell transmission may also help explain why Brass et al. (2009) did not observe a potent antiviral effect of IFITM3 in HeLa-derived cells. Another nonspecific strategy to evade IFITM3 restriction has been described for IAV (Wang et al., 2014), but no direct anti-IFITM3 activity has thus far been identified for any virus. A growing list of viruses has evolved mechanisms to antagonize or degrade various cellular proteins, which offers additional support in favor of their classification as restriction factors (Duggal and Emerman, 2012). The use of HIV-1 mutants carrying mutations in viral accessory or structural genes, as well as IFITM variants containing synthetic or naturally occurring polymorphisms, will reveal potential interactions between HIV-1 and IFITM proteins and their consequences on infection. Furthermore, extending the functional characterization of IFITM proteins beyond humans will allow us to assess whether sequence divergence across taxa may play a role in cross-species virus transmission events.

EXPERIMENTAL PROCEDURES

Cells, Viruses, and Reagents

Primary CD4+ T lymphocytes, MDDCs, and SupT1 and MT4C5 T cell lines were generated and grown as described (Lepelley et al., 2011). pQCXIP plasmids encoding IFITM1, IFITM2, and IFITM3 with N-ter FLAG (FLAG-IFITM) or C-ter FLAG (IFITM-FLAG) were described (Lu et al., 2011). Tet-*ifitm* SupT1 cells were treated with doxycycline (500 ng/ml) overnight to induce FLAG-IFITM as described (Lu et al., 2011). Nevirapine (25 μM) was from the NIH AIDS reagents program. When stated, cells were treated with 500 IU/ml of IFN-α_{2a} (PBL Biomedical Laboratories) and analyzed 48 hr later. The HIV-1 NL4-3 strain, the primary strains DH12, Bx08, and BON, and NL4-3-IRES-GFP have been described (Sourisseau et al., 2007; Lepelley et al., 2011; Wildum et al., 2006). Virus stocks were produced as described (Lepelley et al., 2011).

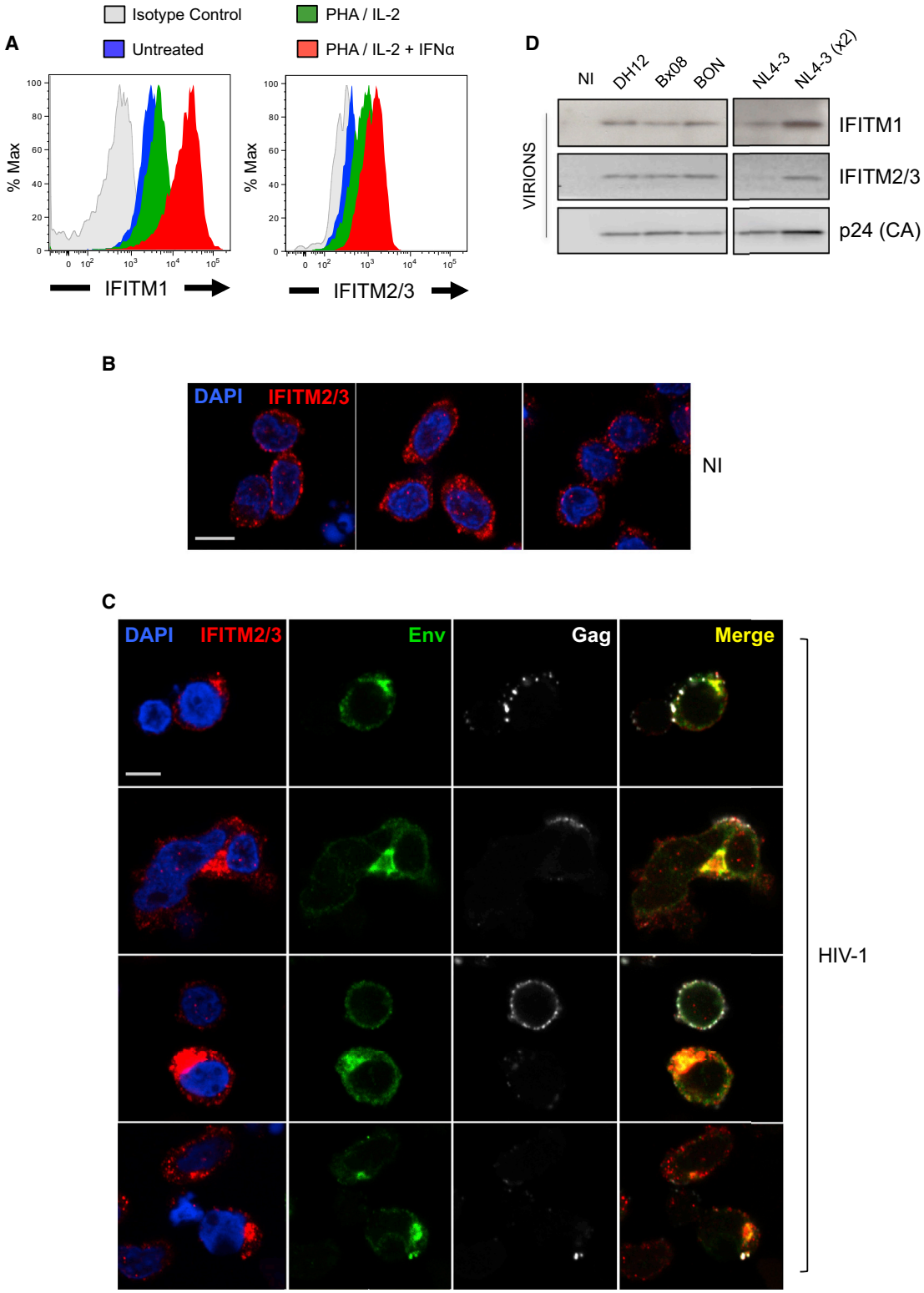

Figure 6. Expression, Localization, and Virion Incorporation of IFITM in Primary T Cells

(A) Nonactivated and PHA-activated CD4+ T cells treated or not treated with IFNα_{2a} for 48 hr were analyzed by flow cytometry to measure IFITM1 and IFITM2/3 levels. One representative experiment among five donors is shown.

(B) Noninfected activated CD4+ T cells were stained with anti-IFITM2/3 (in red). Blue, DAPI (nuclei). Representative fields with cells from three donors are shown.

(legend continued on next page)

Infections and Cell-to-Cell Transmission Assay

SupT1 or primary CD4+ T cells were infected with cell-free virus as described (Lepelley et al., 2011). For the virus cell-to-cell transmission assay utilizing SupT1 as donors, 5×10^6 cells were first infected with 100–200 ng NL4-3 and cultured for 2 days to achieve 30%–50% Gag+ cells. Cells were then induced or not induced for IFITM. A total of 1×10^5 donor cells was mixed with 3×10^5 target SupT1 cells labeled with CellTrace Far Red DDAO-SE (Life Technologies) in 24-well plates. After 2 hr, 2×10^5 target (Far Red+) cells were collected and separated from donors using a FACSAria cell sorter and plated in a 96-well plate. Cells were then analyzed by flow cytometry. When 293T cell were used as donors, 1×10^5 cells were cotransfected in a 24-well plate with the pNL4-3 provirus (1 μg) and FLAG-IFITM (1 μg, unless otherwise stated) using Metafectene transfection reagent (Biontex). A total of 3×10^5 labeled SupT1 targets (~1:3 donor:target) were added 48 hr later. After 2 hr of coculture, targets were manually separated from donors and transferred to a 48-well plate. To measure infectivity, viral particles were purified on a sucrose cushion, and the inoculum (adjusted for p24 content) was added to fresh SupT1 cells. Unless otherwise stated, 25 ng of p24 was added to 10^5 cells. Infection was assessed by measuring the fraction of Gag+ cells after 2–3 days.

Flow Cytometry

The following antibodies were used: IFITM1 (Proteintech, 60074-1-Ig), IFITM2 (Proteintech, 12769-1-AP), IFITM3 (Proteintech, 11714-1-AP), Env (4546, kindly provided by Hugo Mouquet; Malbec et al., 2013), and Gag (KC57, Beckman Coulter). We noticed that rabbit anti-IFITM3 partially cross-reacted with IFITM2, as observed using Tet-*ifitm2* SupT1 cells. Endogenous protein recognized with anti-IFITM3 is thus referred to as IFITM2/3. Anti-Env antibodies were added before fixation. For stainings, cells were fixed with 4% PFA and, when stated, permeabilized with 0.5% saponin. Isotype-matched antibodies were used as negative controls. Samples were analyzed with a FACS Canto II (Becton Dickinson).

Time-Lapse Video Imaging

Cells were plated on Hi-Q^4 microdishes (Ibidi) precoated with 10 μg/ml fibronectin (Sigma). Tet-*ifitm3* SupT1 cells transduced to express actin-mRFP were used as targets. A total of 7×10^5 donor cells infected with HIV-1-IRES-GFP (Wildum et al., 2006) (about 15% of Gag+ cells) was mixed with 7×10^5 cells. Transmission and fluorescence images were taken at 37°C every 5 min up to 60 hr using a Nikon Biostation IMQ, with three fields for each condition. After 60 hr, cells were analyzed by flow cytometry. Images were analyzed using FIJI software. Threshold levels in GFP and RFP were added and used to calculate dual-positive pixels and to determine the area of double GFP/RFP regions per field. Syncytia were visually scored based on their morphology and GFP expression.

Western Blot

Cells were lysed in 1% Triton/PBS in the presence of a protease inhibitor cocktail. Purified virions released from transfected 293T cells and infected SupT1 or primary CD4+ lymphocytes were used to assess protein incorporation. The virus-containing supernatant was overlaid on a 20% sucrose cushion, and particles were pelleted by centrifugation (50,000 × *g*, 4°C) for 90 min. Viral pellets were reoverlaid on a 6% Optiprep cushion and resuspended in lysis buffer. An aliquot was removed for p24 Gag quantification by ELISA, and normalized amounts were loaded for SDS-PAGE. The following antibodies were used: IFITM (see above), FLAG M2 (Sigma), Gag p24 (183-H12-5C), and Env (110H, Institut Pasteur). The purification of HIV-1 particles by velocity gradients was performed as described in the Supplemental Experimental Procedures.

β-Lactamase-Vpr Assay

Viral fusion was assessed as described (Casartelli et al., 2010; Cavrois et al., 2002). Briefly, virions containing the βlam-Vpr fusion protein were produced by cotransfecting 293T cells with a 3:1.5:1 ratio of pNL4-3, FLAG-IFITM3, and βlam-Vpr plasmids, respectively. A total of 25 ng Gag p24 of βlam-Vpr-containing virions was exposed to 1×10^5 SupT1 or MT4C5. After 2 hr, cells were incubated with the CCF2-AM substrate (CCF2-AM kit, Invitrogen) for 2 hr. The cleaved CCF2-AM fluorescence was then measured by flow cytometry. The virus-target cell fusion assay was performed as described (Casartelli et al., 2010).

siRNA Knockdown of IFITM Proteins in HeLa Cells

siRNA (Silencer Select, Ambion) targeted IFITM1 (s16192), IFITM2 (s20771), and IFITM3 (s195035). Silencing in HeLa was performed as described (Lu et al., 2011). A mixture containing 10 nM of each siRNA was used to deplete the three IFITM proteins. Cells were simultaneously exposed to HIV-1(VSV) pseudotypes (5 ng p24/ml in a 12-well plate) in the presence of 500 IU/ml IFN-α_{2a}. After 48 hr, viruses were harvested, and cells were used in coculture assays with SupT1 as targets. IFITM levels were assessed by flow cytometry.

Purification of HIV-1 Particles by Velocity Gradients

Virion purification by Opti-prep fractionation was performed as described (Arenaccio et al., 2014) (Cantin et al., 2008) with minor modifications (Supplemental Experimental Procedures).

Immunogold Labeling of Isolated Viral Particles for Transmission Electron Microscopy

293T cells were cotransfected with a 2:1 ratio of pNL4-3 and pQCXIP IFITM3-FLAG or control plasmid, and supernatants were harvested 48 hr later. Transmission electron microscopy was performed as described (Le Gall et al., 1997) (Shaw et al., 2008), with modifications. Viral particles were concentrated from supernatants by ultracentrifugation over 20% sucrose cushions. Before deposition of the particle suspension on carbon-coated 200 mesh copper palladium grids, the grids were glow discharged in a Quorum Q150R ES (Quorum). After adhesion, particles were chemically fixed with 4% paraformaldehyde in 0.1 M PHEM buffer (pH 7.2). Remaining free aldehydes were quenched with 50 mM NH_4Cl in PBS before labeling with mouse anti-FLAG (M2) antibody (Sigma), followed by a rabbit anti-mouse immunoglobulin G (IgG) (Dako) and 10 nm protein A gold (CMC). After labeling, grids were negatively stained with aqueous 4% uranyl acetate solution and viewed in a Tecnai Spirit electron microscope operated at 120 kV (FEI).

Confocal Immunofluorescent Microscopy

HIV-1-infected CD4+ T cells were fixed, permeabilized, and stained with anti-Gag (mouse anti-p17 ARP342, culture supernatant diluted 1:100; Programme EVA Centre for AIDS Reagents), anti-Env (clone 110H, 50 μg/ml, Institut Pasteur), anti-IFITM1, and anti-IFITM3. Confocal microscopy analysis was carried out on a Zeiss LSM700 using a 63× objective as described (Rudnicka et al., 2009). Representative medial sections are shown. Images were analyzed using FIJI software and assembled with the Magic Montage ImageJ plugin.

Statistical Analysis

Statistical analysis was performed using Prism, using specific tests as indicated in the figure legends.

SUPPLEMENTAL INFORMATION

Supplemental Information includes Supplemental Experimental Procedures, six figures, and one movie and can be found with this article online at http://dx.doi.org/10.1016/j.chom.2014.11.001.

(C) PHA-activated CD4+ T cells were infected with NL4-3 for 3 days and stained with anti-IFITM2/3 (red), anti-Env 110H (green), and anti-p17 Gag (ARP342, recognizing p17 and not the Gag p55 precursor) (white) monoclonal antibodies (mAbs). Representative fields with cells from three independent donors are shown. Scale bar, 5 μm.

(D) PHA-activated CD4+ T cells were infected with DH12, Bx08, and BON primary HIV-1 strains, or with the NL4-3 laboratory-adapted strain, for 3 days. Virions released were purified and analyzed by western blot with the indicated antibodies. One representative experiment is shown, with 1 ng of Gag p24 loaded in each lane. For NL4-3, an additional dose of 2 ng is shown. See also Figure S6.

AUTHOR CONTRIBUTIONS

A.A.C., N.C., and O.S. conceived the study. A.C., T.B., F.P., A.M., M.S., M.E., C.L., N.C., and O.S. performed the experiments and/or participated in the experimental design. C.L. provided vital reagents. A.A.C., N.C., and O.S. wrote and edited the manuscript. All authors approved the final manuscript.

ACKNOWLEDGMENTS

We thank members of the Virus & Immunity Unit for discussions and critical reading of the manuscript. A.A.C. was supported by a postdoctoral fellowship from the Pasteur Foundation. Work was supported by grants from the ANRS, SIDACTION, AREVA Foundation, the Labex IBEID program, the FP7 program, HIT Hidden HIV (Health-F3-2012-305762), and Institut Pasteur, as well as the Vaccine Research Institute, Investissements d'Avenir program (ANR-10-LABX-77). We thank Marine Malbec, Hugo Mouquet, Javier Pizarro-Cerda, the Programme EVA Centre for AIDS Reagents, and the NIH AIDS Reagent Program for the gift of reagents. We also thank Valentina Libri and the Center for Human Immunology for cell sorting.

Received: June 13, 2014
Revised: August 16, 2014
Accepted: October 15, 2014
Published: November 26, 2014

REFERENCES

Accola, M.A., Ohagen, A., and Göttlinger, H.G. (2000). Isolation of human immunodeficiency virus type 1 cores: retention of Vpr in the absence of p6(gag). J. Virol. *74*, 6198–6202.

Amini-Bavil-Olyaee, S., Choi, Y.J., Lee, J.H., Shi, M., Huang, I.C., Farzan, M., and Jung, J.U. (2013). The antiviral effector IFITM3 disrupts intracellular cholesterol homeostasis to block viral entry. Cell Host Microbe *13*, 452–464.

Arenaccio, C., Chiozzini, C., Columba-Cabezas, S., Manfredi, F., Affabris, E., Baur, A., and Federico, M. (2014). Exosomes from human immunodeficiency virus type 1 (HIV-1)-infected cells license quiescent CD4+ T lymphocytes to replicate HIV-1 through a Nef- and ADAM17-dependent mechanism. J. Virol. *88*, 11529–11539.

Bailey, C.C., Huang, I.C., Kam, C., and Farzan, M. (2012). Ifitm3 limits the severity of acute influenza in mice. PLoS Pathog. *8*, e1002909.

Brass, A.L., Huang, I.C., Benita, Y., John, S.P., Krishnan, M.N., Feeley, E.M., Ryan, B.J., Weyer, J.L., van der Weyden, L., Fikrig, E., et al. (2009). The IFITM proteins mediate cellular resistance to influenza A H1N1 virus, West Nile virus, and dengue virus. Cell *139*, 1243–1254.

Cantin, R., Diou, J., Bélanger, D., Tremblay, A.M., and Gilbert, C. (2008). Discrimination between exosomes and HIV-1: purification of both vesicles from cell-free supernatants. J. Immunol. Methods *338*, 21–30.

Casartelli, N., Sourisseau, M., Feldmann, J., Guivel-Benhassine, F., Mallet, A., Marcelin, A.G., Guatelli, J., and Schwartz, O. (2010). Tetherin restricts productive HIV-1 cell-to-cell transmission. PLoS Pathog. *6*, e1000955.

Cavrois, M., De Noronha, C., and Greene, W.C. (2002). A sensitive and specific enzyme-based assay detecting HIV-1 virion fusion in primary T lymphocytes. Nat. Biotechnol. *20*, 1151–1154.

Chesarino, N.M., McMichael, T.M., Hach, J.C., and Yount, J.S. (2014). Phosphorylation of the antiviral protein interferon-inducible transmembrane protein 3 (IFITM3) dually regulates its endocytosis and ubiquitination. J. Biol. Chem. *289*, 11986–11992.

Chutiwitoonchai, N., Hiyoshi, M., Hiyoshi-Yoshidomi, Y., Hashimoto, M., Tokunaga, K., and Suzu, S. (2013). Characteristics of IFITM, the newly identified IFN-inducible anti-HIV-1 family proteins. Microbes Infect. *15*, 280–290.

Dale, B.M., Alvarez, R.A., and Chen, B.K. (2013). Mechanisms of enhanced HIV spread through T-cell virological synapses. Immunol. Rev. *251*, 113–124.

Deneka, M., Pelchen-Matthews, A., Byland, R., Ruiz-Mateos, E., and Marsh, M. (2007). In macrophages, HIV-1 assembles into an intracellular plasma membrane domain containing the tetraspanins CD81, CD9, and CD53. J. Cell Biol. *177*, 329–341.

Desai, T.M., Marin, M., Chin, C.R., Savidis, G., Brass, A.L., and Melikyan, G.B. (2014). IFITM3 restricts influenza A virus entry by blocking the formation of fusion pores following virus-endosome hemifusion. PLoS Pathog. *10*, e1004048.

Diamond, M.S., and Farzan, M. (2013). The broad-spectrum antiviral functions of IFIT and IFITM proteins. Nat. Rev. Immunol. *13*, 46–57.

Ding, S., Pan, Q., Liu, S.-L., and Liang, C. (2014). HIV-1 mutates to evade IFITM1 restriction. Virology *454-455*, 11–24.

Duggal, N.K., and Emerman, M. (2012). Evolutionary conflicts between viruses and restriction factors shape immunity. Nat. Rev. Immunol. *12*, 687–695.

Everitt, A.R., Clare, S., Pertel, T., John, S.P., Wash, R.S., Smith, S.E., Chin, C.R., Feeley, E.M., Sims, J.S., Adams, D.J., et al.; GenISIS Investigators; MOSAIC Investigators (2012). IFITM3 restricts the morbidity and mortality associated with influenza. Nature *484*, 519–523.

Feeley, E.M., Sims, J.S., John, S.P., Chin, C.R., Pertel, T., Chen, L.-M., Gaiha, G.D., Ryan, B.J., Donis, R.O., Elledge, S.J., and Brass, A.L. (2011). IFITM3 inhibits influenza A virus infection by preventing cytosolic entry. PLoS Pathog. *7*, e1002337.

Haller, O. (2013). Dynamins are forever: MxB inhibits HIV-1. Cell Host Microbe *14*, 371–373.

Hickford, D., Frankenberg, S., Shaw, G., and Renfree, M.B. (2012). Evolution of vertebrate interferon inducible transmembrane proteins. BMC Genomics *13*, 155.

Huang, I.C., Bailey, C.C., Weyer, J.L., Radoshitzky, S.R., Becker, M.M., Chiang, J.J., Brass, A.L., Ahmed, A.A., Chi, X., Dong, L., et al. (2011). Distinct patterns of IFITM-mediated restriction of filoviruses, SARS coronavirus, and influenza A virus. PLoS Pathog. *7*, e1001258.

Jia, R., Pan, Q., Ding, S., Rong, L., Liu, S.L., Geng, Y., Qiao, W., and Liang, C. (2012). The N-terminal region of IFITM3 modulates its antiviral activity by regulating IFITM3 cellular localization. J. Virol. *86*, 13697–13707.

Jia, R., Xu, F., Qian, J., Yao, Y., Miao, C., Zheng, Y.-M., Liu, S.-L., Guo, F., Geng, Y., Qiao, W., and Liang, C. (2014). Identification of an endocytic signal essential for the antiviral action of IFITM3. Cell. Microbiol. *16*, 1080–1093.

John, S.P., Chin, C.R., Perreira, J.M., Feeley, E.M., Aker, A.M., Savidis, G., Smith, S.E., Elia, A.E.H., Everitt, A.R., Vora, M., et al. (2013). The CD225 domain of IFITM3 is required for both IFITM protein association and inhibition of influenza A virus and dengue virus replication. J. Virol. *87*, 7837–7852.

Jouve, M., Sol-Foulon, N., Watson, S., Schwartz, O., and Benaroch, P. (2007). HIV-1 buds and accumulates in "nonacidic" endosomes of macrophages. Cell Host Microbe *2*, 85–95.

Laguette, N., and Benkirane, M. (2012). How SAMHD1 changes our view of viral restriction. Trends Immunol. *33*, 26–33.

Le Gall, S., Prevost, M.C., Heard, J.M., and Schwartz, O. (1997). Human immunodeficiency virus type I Nef independently affects virion incorporation of major histocompatibility complex class I molecules and virus infectivity. Virology *229*, 295–301.

Lepelley, A., Louis, S., Sourisseau, M., Law, H.K., Pothlichet, J., Schilte, C., Chaperot, L., Plumas, J., Randall, R.E., Si-Tahar, M., et al. (2011). Innate sensing of HIV-infected cells. PLoS Pathog. *7*, e1001284.

Li, K., Markosyan, R.M., Zheng, Y.-M., Golfetto, O., Bungart, B., Li, M., Ding, S., He, Y., Liang, C., Lee, J.C., et al. (2013). IFITM proteins restrict viral membrane hemifusion. PLoS Pathog. *9*, e1003124.

Lin, T.-Y., Chin, C.R., Everitt, A.R., Clare, S., Perreira, J.M., Savidis, G., Aker, A.M., John, S.P., Sarlah, D., Carreira, E.M., et al. (2013). Amphotericin B increases influenza A virus infection by preventing IFITM3-mediated restriction. Cell Rep. *5*, 895–908.

Lu, J., Pan, Q., Rong, L., He, W., Liu, S.L., and Liang, C. (2011). The IFITM proteins inhibit HIV-1 infection. J. Virol. *85*, 2126–2137.

Malbec, M., Porrot, F., Rua, R., Horwitz, J., Klein, F., Halper-Stromberg, A., Scheid, J.F., Eden, C., Mouquet, H., Nussenzweig, M.C., and Schwartz, O. (2013). Broadly neutralizing antibodies that inhibit HIV-1 cell to cell transmission. J. Exp. Med. *210*, 2813–2821.

Malim, M.H., and Bieniasz, P.D. (2012). HIV restriction factors and mechanisms of evasion. Cold Spring Harb Perspect Med *2*, a006940.

Mudhasani, R., Tran, J.P., Retterer, C., Radoshitzky, S.R., Kota, K.P., Altamura, L.A., Smith, J.M., Packard, B.Z., Kuhn, J.H., Costantino, J., et al. (2013). IFITM-2 and IFITM-3 but not IFITM-1 restrict Rift Valley fever virus. J. Virol. *87*, 8451–8464.

Murooka, T.T., Deruaz, M., Marangoni, F., Vrbanac, V.D., Seung, E., von Andrian, U.H., Tager, A.M., Luster, A.D., and Mempel, T.R. (2012). HIV-infected T cells are migratory vehicles for viral dissemination. Nature *490*, 283–287.

Perreira, J.M., Chin, C.R., Feeley, E.M., and Brass, A.L. (2013). IFITMs restrict the replication of multiple pathogenic viruses. J. Mol. Biol. *425*, 4937–4955.

Raposo, R.A.S., Abdel-Mohsen, M., Bilska, M., Montefiori, D.C., Nixon, D.F., and Pillai, S.K. (2013). Effects of cellular activation on anti-HIV-1 restriction factor expression profile in primary cells. J. Virol. *87*, 11924–11929.

Roesch, F., Meziane, O., Kula, A., Nisole, S., Porrot, F., Anderson, I., Mammano, F., Fassati, A., Marcello, A., Benkirane, M., and Schwartz, O. (2012). Hyperthermia stimulates HIV-1 replication. PLoS Pathog. *8*, e1002792.

Rudnicka, D., Feldmann, J., Porrot, F., Wietgrefe, S., Guadagnini, S., Prévost, M.C., Estaquier, J., Haase, A.T., Sol-Foulon, N., and Schwartz, O. (2009). Simultaneous cell-to-cell transmission of human immunodeficiency virus to multiple targets through polysynapses. J. Virol. *83*, 6234–6246.

Sattentau, Q.J. (2011). The direct passage of animal viruses between cells. Curr Opin Virol *1*, 396–402.

Shaw, M.L., Stone, K.L., Colangelo, C.M., Gulcicek, E.E., and Palese, P. (2008). Cellular proteins in influenza virus particles. PLoS Pathog. *4*, e1000085.

Siegrist, F., Ebeling, M., and Certa, U. (2011). The small interferon-induced transmembrane genes and proteins. J. Interferon Cytokine Res. *31*, 183–197.

Smith, S., Weston, S., Kellam, P., and Marsh, M. (2014). IFITM proteins-cellular inhibitors of viral entry. Curr Opin Virol *4*, 71–77.

Sourisseau, M., Sol-Foulon, N., Porrot, F., Blanchet, F., and Schwartz, O. (2007). Inefficient human immunodeficiency virus replication in mobile lymphocytes. J. Virol. *81*, 1000–1012.

Sundquist, W.I., and Kräusslich, H.G. (2012). HIV-1 assembly, budding, and maturation. Cold Spring Harb Perspect Med *2*, a006924.

Tang, Y., Leao, I.C., Coleman, E.M., Broughton, R.S., and Hildreth, J.E.K. (2009). Deficiency of niemann-pick type C-1 protein impairs release of human immunodeficiency virus type 1 and results in Gag accumulation in late endosomal/lysosomal compartments. J. Virol. *83*, 7982–7995.

Wang, S., Chi, X., Wei, H., Chen, Y., Chen, Z., Huang, S., and Chen, J.L. (2014). Influenza A virus-induced degradation of eukaryotic translation initiation factor 4B contributes to viral replication by suppressing IFITM3 protein expression. J. Virol. *88*, 8375–8385.

Welsch, S., Keppler, O.T., Habermann, A., Allespach, I., Krijnse-Locker, J., and Kräusslich, H.G. (2007). HIV-1 buds predominantly at the plasma membrane of primary human macrophages. PLoS Pathog. *3*, e36.

Weston, S., Czieso, S., White, I.J., Smith, S.E., Kellam, P., and Marsh, M. (2014). A membrane topology model for human interferon inducible transmembrane protein 1. PLoS ONE *9*, e104341.

Wildum, S., Schindler, M., Münch, J., and Kirchhoff, F. (2006). Contribution of Vpu, Env, and Nef to CD4 down-modulation and resistance of human immunodeficiency virus type 1-infected T cells to superinfection. J. Virol. *80*, 8047–8059.

Yount, J.S., Moltedo, B., Yang, Y.-Y., Charron, G., Moran, T.M., López, C.B., and Hang, H.C. (2010). Palmitoylome profiling reveals S-palmitoylation-dependent antiviral activity of IFITM3. Nat. Chem. Biol. *6*, 610–614.